Virology 513 (2018) 85–90

Contents lists available at ScienceDirect

Virology

journal homepage: www.elsevier.com/locate/virology

An easy way to detect dengue virus using nanoparticle-antibody conjugates

Caroline R. Basso[a], Claudia C. Tozato[b], Bruno P. Crulhas[a], Gustavo R. Castro[a], João Pessoa A. Junior[b], Valber A. Pedrosa[a,*]

[a] Department of Chemistry and Biochemistry, Institute of Bioscience, UNESP-Botucatu, SP 18618-000, Brazil
[b] Department of Microbiology and Immunology, Institute of Bioscience, UNESP-Botucatu, SP 18618-000, Brazil

ARTICLE INFO

Keywords:
Infectious diagnostics
Biosensor
Fast detection

ABSTRACT

The aim of the present research is to propose a new method based on localized surface plasmon resonance (LSPR) for fast dengue virus detection. A pool with four dengue serotypes (DENV-1, -2, -3, -4) was detected through antigen-antibody binding using gold nanoparticles (AuNPs) as signaling antibody carriers. Such result was confirmed through surface plasmon resonance (SPR), transmission electron microcopy (TEM), and dynamic light scattering (DLS) techniques. The limit of detection was calculated for $TCID_{50}$ 10^7 demonstrating a linear correlation between viral concentration and number of cells with an r^2 value of > 0.993. The assay presented good sensibility and reproducibility of results and the negative controls were not mistakenly detected. This design requires no pretreatment or high trained person. In the future, it can be used in commercial antibody detection kits.

1. Introduction

Dengue is an infectious viral disease caused by one of its four distinct serotypes (DENV-1, -2, -3 or -4). This is a flavivirus (belonging to family *Flaviviridae*) transmitted to humans through the bite of female mosquitoes belonging to the species *Aedes aegypti* and, to a lesser extent, through the bite of *Aedes albopictus* female mosquitoes (Jahanshahi et al., 2014). The genetic material of the dengue virus, RNA positive-sense single-strand containing approximately 10,700 bases, encodes three structural proteins (capsid [C], membrane protein [M] and glycoprotein for viral envelope [E]) and seven nonstructural proteins (NS1, NS2a, NS2b, NS3, NS4a, NS4b and NS5) (Ramos-Castañeda et al., 2017). Data from the World Health Organization (WHO) indicate that the dengue virus remains a major health problem in tropical and subtropical regions worldwide. It leads to 390 million dengue infections per year, and 96 million clinical manifestations of the disease. Estimates foresee that 3.9 billion people are at risk of dengue virus infection in 128 countries (Ramos-Castañeda et al., 2017; World Health Organization, 2017). The dengue virus causes dengue fever (DF), which main symptoms are: high fever (40 °C/104 °F), severe headache; pain behind the eyeballs, in the muscles and joints; nausea; vomiting; swollen glands or rash. It can develop into dengue hemorrhagic fever (DHF) and dengue shock syndrome (DSS) (Kumbhat et al., 2010). These symptoms are reported approximately 10 days after virus inoculation in humans. The virus incubation period in the host lasts from 4 to 10 days. Infection with one of four dengue serotypes DENV 1–4 leads to life-long protective immunity against this serotype, but only partial cross-protection against the other serotypes. For example, if a person contracts DENV 1, they may still be infected with DENV 2, 3 and 4 throughout their lifetime (Zhang et al., 2015).

The dengue virus diagnosis is primarily done through the clinical signs presented by the patient and It is confirmed through laboratory tests such as Immunoglobulin M (IgM) and Immunoglobulin G (IgG) (Nunes et al., 2011; Wang and Sekaran, 2010), enzyme-linked immune sorbent assay (ELISA) (Wiwanitkit and Wiwanitkit, 2015), reverse transcription polymerase chain reaction (RT-PCR) (Saxena et al., 2008) and non-structural protein 1 (NS1) detection and point-of-care (POC) test (Jahanshahi et al., 2014). However, none of these exams are fast, specific and sensitive enough to be used as stand-alone diagnostic tool, and some of them require few days to get the results, besides their high cost (Wiwanitkit and Wiwanitkit, 2015; Saxena et al., 2008; Guzman and Kouri, 2004). Moreover, the requirement for specialized training and equipment and time consuming nature of these assays limits their widespread utility for virus detection, compromising the rapid diagnosis of viral infections.

Recently the use of nanotechnologies for the development of biosensors has been gaining more space by significantly optimizing the sample volume used, the time of analysis, the limit of detection and the possible detection of analytes in unusable samples in classical methods. The use nanoparticles makes it possible to detect infectious diseases

* Corresponding author.
E-mail address: vpedrosa@ibb.unesp.br (V.A. Pedrosa).

http://dx.doi.org/10.1016/j.virol.2017.10.001
Received 24 August 2017; Received in revised form 28 September 2017; Accepted 2 October 2017
Available online 14 October 2017

outside laboratories in a more sensitive, economical and fast way, because they present high specificity to different pathogens (Vaculovicova et al., 2017). The development of assays based on metallic nanoparticles has been widely used to diagnose human-related diseases (Urdea et al., 2006). The gold nanoparticles (AuNPs) have attracted the attention of researchers, and used as diagnostic apparatus due to their easy synthesis, low cost, simplicity, practicality, size, shape, optical properties and to the functionality of their surface (antibodies, enzymes, aptamers, nucleic acids) (Basso et al., 2015; Cordeiro et al., 2016). The use of gold in immunoassay production differs from the use of other materials due to its high sensitivity and to the collective oscillation of gold atoms' conductive electrons, known as localized surface plasmon resonance (LSPR) (Cordeiro et al., 2016; Pelton et al., 2008). The LSPR is formed by two plasmon absorption bands; the first one refers to the longitudinal plasmon, which is responsible for light scattering and absorption along the long axis of the particle. This axis is related to the visible region of IR, which stays close to the electromagnetic spectrum. The other band corresponds to the transverse plasmon, which is responsible for light scattering and absorption along the short axis of the particle. Often, the gold nanoparticles in the visible region of the electromagnetic spectrum show maximum absorption at ca 520 nm in this region of the particle (Basso et al., 2015; Cordeiro et al., 2016; Pelton et al., 2008; Wang and Irudayaraj, 2008). The AuNPs solution gets an intense red color when it is dispersed. The extinction band redshifts generated a bluish/purple solution after bioconjugation, due to the formation of aggregates (Liu et al., 2013). This visual change in the color has been used in the development of several visual colorimetric biosensors applied to detect: Alzheimer disease (Cao et al., 2011), *Mycoplasma pneumonia* (Xianyu et al., 2014), and bacteriophages (Endo et al., 2005). It is also used to detect a prostate specific antigen (PSA) and HIV-associated protein (Rica and Stevens, 2012), *E. coli* and *Salmonella* (Ma and Sui, 2002), influenza virus (Li et al., 2007), and to detect analytes from nucleic acids of small molecules (Wang et al., 2009), nuclease activity (Haes et al., 2005), immunoglobulin (Tang et al., 2013) and pathogens (Wang and Irudayaraj, 2008). The noble metal solution can also be quantitatively measured in an ultraviolet-visible (UV–Vis) spectrophotometer in order to generate higher sensitivity and lower detection limits (Liu et al., 2011).

The aim of the present study is to propose a new, simpler and easier methodology for early detection of dengue virus through LSPR immunosensors. The methodology allows detecting all four dengue serotypes presenting high specificity and selectivity. The biosensor principle and format is shown in Fig. 1. Our innovative system should be a helpful tool for the detection of DENV since it solves many of the limitations of current virus detection. This immunosensor and subsequent analysis is cost effective, simple to perform, and the assay components are highly stable at temperatures above 30 °C enabling easy storage at room temperature

2. Experiments

2.1. Materials

The following materials were purchased at Sigma-Aldrich (USA): 11-mercaptoundecanoid acid, 95% (MUA); N-hydroxysuccinimide (NHS) 98% and N-(3-dimethylaminopropyl)-N′ethylcarbodiimide hydrochloride (EDC); phosphate-buffered saline (PBS); sodium citrate dehydrate 99%; gold (III) chloride trihydrate 99.99% ($HAuCl_4$); absolute ethanol 99%; bovine serum albumin solution (BSA) 98% (1 mg/mL^{-1} in 10 mM PBS, pH 7.4); and glycine–HCl (pH 3.0). The water used in all solution preparations came from a Millipore unit (USA). All working solutions were prepared with analytical grade chemicals.

The monoclonal antibody [D1-11(3)] of the dengue virus types 1, 2, 3 and 4 were purchased at GeneTex (USA). Mice were immunized with a mixture of dengue 1, 2, 3 and 4. Spleen cells were used to prepare hybridomas and clones selected based on the ability of the antibody they produced to react with each dengue serotype (datasheet provided by the manufacturer). The antibody was chosen from the ability to react with the different serotypes.

2.2. Instruments

The UV–Vis absorption spectra were collected in a Biochrom Lira S11 spectrophotometer (Biochrom Ltd, England) at 1 cm glass cell, wavelength 400–800 nm, with 1 nm step; speed 500 nm min^{-1}, and wavelength accuracy of 0.5 nm. The molecular interactions between the monoclonal antibody and the dengue virus were investigated through Surface Plasmon Resonance (SPR) (AutoLab Springle®, Eco-Chemie, Netherlands). The planar gold sensor SPR discs (17 mm diameter) were purchased from Autolab. All experiments were carried out at 22 °C. The AuNPs diameter and their dispersity in solution were analyzed through dynamic light scattering (DLS) in a DynaPro Titan apparatus (Wyatt Technology Corporation). This technique made it possible estimating the hydrodynamic radius of the particles. Samples were filtered in 0.22 μm Millex-GV filters (Millipore®).

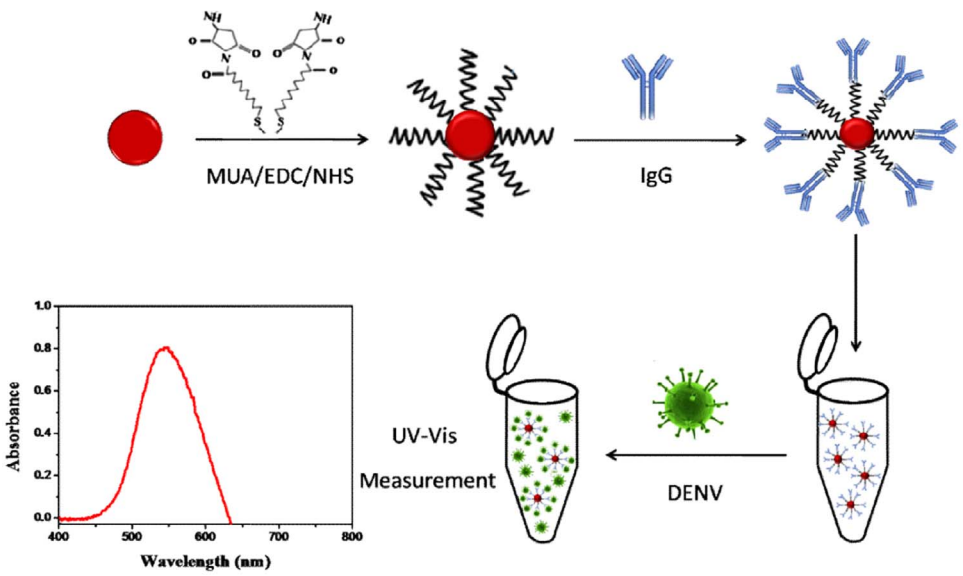

Fig. 1. Schematic representation of the detection of the dengue virus. The design shows the surface modification of the AuNP with the formation of the self-assembled monolayers conjugated to the antibodies for virus detection demonstrated by the UV–Vis spectrum.

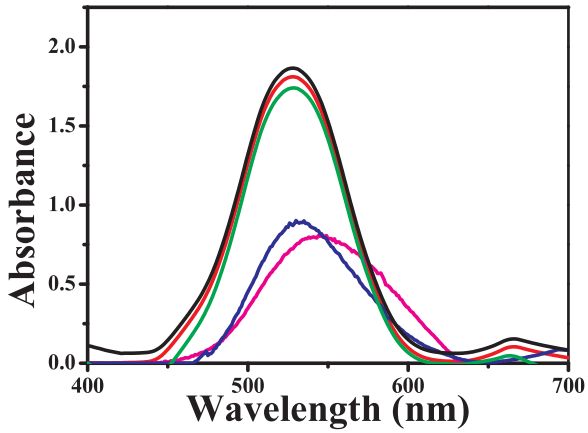

Fig. 2. UV–Vis spectrum showing the absorbance of all modification steps: AuNPs (black line), MUA (red line), EDC-NHS (green line), antibody (blue line) and pool of DENV (pink line).

2.3. Gold nanoparticles preparation and surface modification

The schematic representation of the steps used to assemble the assay can be seen in Fig. 1. The AuNPs were prepared through the reduction of the $HAuCl_4$ complex as Au^{3+} ions into Au° using citrate ions. As previously reported, these ions were reducing and capping agents (Wang and Irudayaraj, 2008). The final gold nanoparticles solution showed concentration 0.1 g L^{-1}. The preparation of the AuNPs samples to be viewed in TEM was performed in 3-mm copper grid, Fig. S1. The grid was covered with carbon and placed over a drop of AuNPs solution, for 10 min. Subsequently, it was left to dry on paper filter in order to be analyzed in the following day. The particle size of the gold colloid was measured by the aspect ratios of the gold nanoparticles and their modification were determined through transmission electron microcopy (TEM) images, which were acquired in a Tecnai Spirit (Fei Company-USA), and the results were analyzed in the ImageJ software. The nanoparticle has as 22 nm with a standard deviation of 5.0 nm. The particles were roughly spherical and approximately normally distributed. The size measurement was repeated several times and no significant difference in size was found, indicating a stable colloid. The concentration of the colloid was found by assuming complete reduction of the $HAuCl_4$ (Frens, 1973). The mass concentration of gold in all batches was 420 μg/mL, and for 22 nm diameter particles, a molar particle concentration of 0.7 nM.

The AuNPs surface modification was performed through the deposition of self-assembled monolayer (SAM) using MUA. In order to achieve such modification, 100 μL of 0.018 mol L^{-1} of MUA were added to 2 mL of AuNPs solution and left to rest for 1 h. The linkers' terminal carboxylic groups were activated in 200 μL of a 1:1 mixture containing 0.4 mol L^{-1} of EDC and 0.1 mol L^{-1} of NHS, for 1 h. This procedure triggered covalent bonds with the antibodies' amines. It was, then, added with 100 μL of antibody 1 μg/mL.

2.4. Dengue and zika samples

Samples of the four dengue serotypes and zika virus were collected in the virology research laboratory of the Infectious and Parasitic Diseases Department at Medical School of São José do Rio Preto (Brazil). All samples were cultured in C6-36 cell line using Leibovitz's medium (L-15) added with 10% tryptose phosphate broth and 10% fetal bovine serum (fbs), at 28 °C. Fig. S2 shows images of cell cultures of both viruses. Cells were infected, separately, with each type DENV virus. Virus titers were expressed as tissue culture infectious dose, expressed as $TCID_{50}$ units per mL with serial dilutions of DENV 1–4 serotypes. Cells were cultured in 96-well culture plates with 200 μL of L-15 medium and fbs with density of 5×10^5 cells/well. At about 80% confluence around 24 h later at 28 °C, ten-fold serial dilution of the four serotypes was done. As control was used just C6-36 cells without the virus. Plates for each serotype were made in triplicate and stored at 28 °C. The cytopathic effect was observed daily using an inverted microscopy for 7 days. After this period infected fields were counted and 50% tissue culture infectious dose ($TCID_{50}$) of each virus was calculated according Kulkarni et al. (Reed and Muench, 1938). The samples also were previously tested through the RT-qPCR technique.

2.5. Determination of dengue

One hundred microliters (100 μL) from the pool containing four dengue serotypes (DENV 1, 2, 3 and 4) or negative control (zika virus or yellow fever vaccine)with a average titre of $TCID_{50}$ 10^7 were added to 900 microliters AuNPs-antibody complex mixed at 25 °C for 3 min. UV/Vis spectrophotometric analysis was performed using the Biochrom Lira S11. All experiments were performed in compliance with institutional biosafety committee guidelines. The appropriate authorities kindly approved the experimental study.

3. Results and discussion

3.1. Microstructure characterization

The dengue antibodies were labeled according to the AuNPs. It was done by taking advantage of the electrostatic and covalent interactions between the antibody side chains and the nanoparticle surfaces. Fig. 2 shows all steps of the AuNPs surface modifications monitored through LSPR spectroscopy techniques. Each absorbance peak reduction and the shifts in wavelength observed through this technique changed the AuNP surface (Wang and Irudayaraj, 2008). The bare gold colloids presented extinction peak at 524 nm (black line). The extinction shifted 3 nm to red and gave final λ_{max} 527 nm (red line) through the MUA adsorption, thus indicating formatting of self-assembled monolayers to the colloid surface. The SAM consisted of a thiol group, whose end was connected to AuNPs, which contained an -SH group bonded to a carbon atom. Its other end presented a carboxylic group, which was activated by an EDC-NHS solution and triggered covalent bonds with the antibodies' amines. After a new reduction in the absorbance peak was activated, the shift in the wavelength underwent a 2 nm increase, thus going to 529 nm (green line). Covalent bindings between the antibodies' amine and the AuNPs mediated by the self-organized monolayers took place when the antibody was added. The graph shows the 4-nm shift (533 nm) in the wavelength when it was compared to the modification accomplished through EDC-NHS (blue line). A pool of dengue virus serotypes (1, 2, 3 and 4) was added in order to show the ability of these gold nanoparticle-conjugated antibodies to bind to an antigen. The 14-nm shift resulted from the increased local refractive index caused by the antigen-antibody binding (pink line).

The dynamic range of this signal was found as a way to optimize the antibody concentration. The LSPR shift upon antibody binding was measured for different antibody and antigen concentrations. Higher antibody concentrations led to lower absorbance peaks (Fig. 3). Such behavior resulted from the larger surface area of the gold nanoparticles, which were covered with the antibodies, thereby, preventing the gold surface interaction with the transmitted light (Wang and Irudayaraj, 2008). The lowest concentration 0.5 μg/mL led to 0.85 absorbance (black line) and the higher concentration 1.5 μg/mL (red line) has decreased the absorbance peak, thus indicating surface reduction in the nanoparticles exposed to interaction with light. The LSPR bands kept on loosing intensity and the antibody concentrations increased. The green line showed concentration 2.5 μg/mL and absorbance 0.79; the blue line concerned concentration 5.0 μg/mL and absorbance 0.74 μg/mL; and the pink line showed the highest concentration (10.0 μg/mL) and the lowest absorbance peak (0.73). There was no significant difference in the intensity reduction of the LSPR band at the two highest

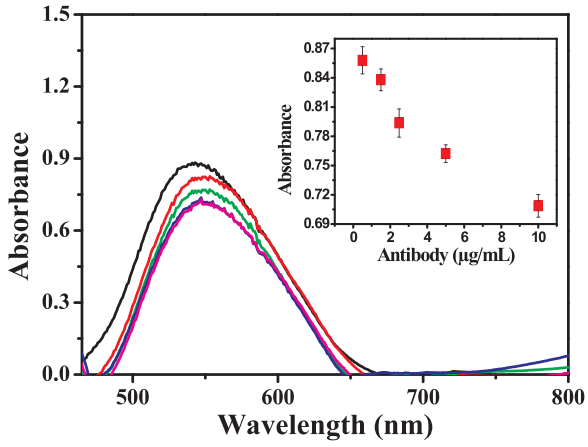

Fig. 3. Variations of antibodies concentrations. 0.5 µg/mL (black line), 1.5 µg/mL (red line), 2.5 µg/mL (green line), 5.0 µg/mL (blue line) and 10.0 µg/mL (pink line), all dilutions were made in PBS. Insert in figure: Calibration curve with R^2: 0.91.

concentrations (5.0 µg/mL and 10.0 µg/mL); which showed total attachment of anti-DENV to the surface of the AuNPs. The insert of Fig. 3 shows the calibration curve of five different IgG antibody concentrations. The absorbance intensity peak decreased as the concentration increased; the system saturated at concentration 5 µg/mL. The dissociation constant was set in the autolab software. The k_a was found through the slope of a SPR signal plot of the antibody *vs* virus concentration, wherein k_a was 0.7 × 105 mol L^{-1}. We made the option for using concentration 0.5 µg/mL (lowest concentration tested) in order to avoid wasting unreacted signaling antibodies, as well as to improve test sensitivity and to prevent extra costs caused by reduced unreacted signaling antibody wastes.

The data in Fig. 3 also were used to calculate the antibody coverage on the gold at the different bulk antibody concentrations. Equations for the change in peak absorbance (ΔA) with coating can be calculated using de Feijter's formula (De Feijter et al., 1978):

$$\Gamma = s\frac{ns - mn}{dn/dc}$$

where mass of protein absorbed per unit area (coverage, Γ), n is the refractive index for the shell (ns) and the surrounding medium (n_m), which in this system is essentially water, which has a refractive index of 1.39 at 550 nm, and dn/dc used as refractive index increment of 0.19 mL g^{-1} for protein (Zhao et al., 2011; Kaur and Forrest, 2012). These correspond to between 6 and 25 antibody molecules per gold particle.

The surface morphology of the nanostructures was recorded through transmission electron microscopy. Fig. 4A shows the AuNPs without modifications and 22 nm diameter, on average. The antibodies' immobilization on AuNPs involved locally depositing self-assembled monolayer on the surface. The formation of SAMs with MUA promotes an asymmetric shape of nanoparticles and an increased diameter mean in the nanostructures (34 nm) (Fig. 4B). The amines found in the antibodies covalently bound to the thiol groups gathered on the surface of the AuNPS causing the appearance of an ellipse. The AuNPs provided a stable solution and did not form colloid aggregation (Fig. 4C). After the DENV-antibody interaction, the AuNPs showed diameter 126 nm (Fig. 4D). The dengue virus consists of a ribonucleoprotein core and of lipoproteins envelops with virion (50 nm diameter) (Gromowski et al., 2010). The results found through the TEM technique were consistent with those found through UV–VIs. The reduction, along with the shift at the LSPR band peak, showed all chemical bonds and modifications occurring throughout the experiment. The results obtained by TEM were similar to those shown in previously published studies about the canine distemper virus (CDV) and bacteria (*Lactobacillus* spp. and *Staphylococcus aureus*) detection, thus evidencing the high specificity of the herein used methodology (Basso et al., 2015; Cordeiro et al., 2016; Pelton et al., 2008; Wang and Irudayaraj, 2008; Liu et al., 2013, 2011; Cao et al., 2011; Xianyu et al., 2014; Endo et al., 2005; Rica and Stevens, 2012; Ma and Sui, 2002; Li et al., 2007; Wang et al., 2009; Haes et al., 2005; Tang et al., 2013; Frens, 1973; Reed and Muench, 1938; De Feijter et al., 1978; Zhao et al., 2011; Kaur and Forrest, 2012; Gromowski et al., 2010; Verdoodt et al., 2017).

3.2. SPR experiments

Once the assay conditions were optimized, the procedure was conducted in order to detect the dengue virus through the surface plasmon resonance technique. The SPR combines the molecular recognition of biomolecules and the high selectivity of the equipment. The results have shown all the molecules' adsorption and desorption process on the surface of the gold sensor. Fig. 5 shows the SPR graph with SPR response (RU) on the y-axis indicating the amount of adsorbed material on the sensor surface and the time of the experiment in seconds on the x-axis and it corroborates the whole binding process on the AuNPs surface. The surface modification in the sensor was triggered by the injection of the MUA solution, which was left overnight to form self-assembled monolayers. The baseline was performed through the addition of phosphate buffer solution pH 7.4 (PBS). The injection of EDC-NHS activated the carboxyl groups of MUA and triggered covalent bonds with the antibodies' amines (point A). The elapsed time of each injection in the experiment was performed by washing it in PBS to remove the excess of unbound material (blue arrows downwards). The addition of the antibody solution to the gold sensor surface (point B) lasted 40 min. After the washing process, when we subtracted point B from the drop in the graphic, we found RU change of 2096 millidegrees, which corresponded to 17.5 ng mm^{-2} of antibodies adsorption on the sensor's surface. Each 120 millidegrees in the plasmon resonance angle is equivalent to 1 ng mm^{-2} adsorbed material in the sensor layer (Basso et al., 2015). The injection of the BSA 1 mg/mL^{-1} solution at point C was performed in order to block the remaining spaces between the antibodies, thereby, preventing the direct bonding of the sample to the sensor's surface. The injection of the dengue virus pool (serotypes 1, 2, 3 and 4) was done at point D. After the washing in PBS (blue arrow downwards), there was small decrease in the signal in comparison to the injection point, which confirms the specific binding antigen-antibody. The glicine-HCL solution was added in order to maintain the reproducibility in the experiment and to regenerate the sensor's surface. This solution only broke the antigen-antibody binding (pink line upwards). Points E and G referred to the injection of the dengue virus pool and showed the reproducibility of the results found throughout the experiment. It was possible observing small decrease in the signal after the washing steps (blue arrows down wards), which highlighted the binding antigen-antibody. The negative control was performed through the injection of a zika virus sample (point F) after the PBS washing (blue arrow downwards). There was a total line decrease equaling the baseline, and it showed no binding between the sample and the antibody. The zika virus sample was once more added to the sensor in order to confirm the specificity of antibody binding to the dengue virus pool. We observed a total decrease in the signal after the PBS washing and it showed the absence of bindings (point H and blue arrow down wards). All washing steps in the experiment were performed through PBS at pH 7.4; they were represented by the blue arrows pointing downwards. Every step of the sensor's surface regeneration was performed using glycine-HCl solution after each sample was washed in order to break the antigen-antibody binding, which was highlighted by the pink arrows pointing upwards.

3.3. Analytical performance

To evaluate the sensitivity and dynamic range of the immunosensor, analytical routine were carried out under optimal conditions. We found

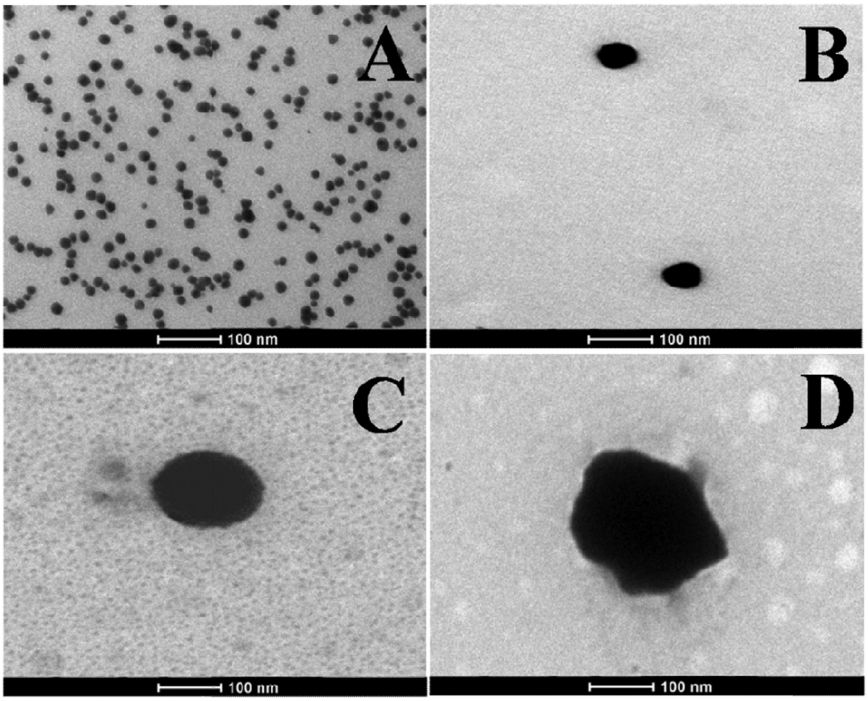

Fig. 4. TEM imagens with a scale of 100 nm. AuNPs (A), AuNPs modified with MUA and EDC-NHS (B), AuNPs modified with MUA/EDC-NHS and antibody (C) and AuNPs modified with MUA/EDC-NHS and antibody bound to the DENV.Down arrows (blue line) indicate wash step using tween/PBS, and up Arrows (pink line) indicate injection of glycine-HCl.

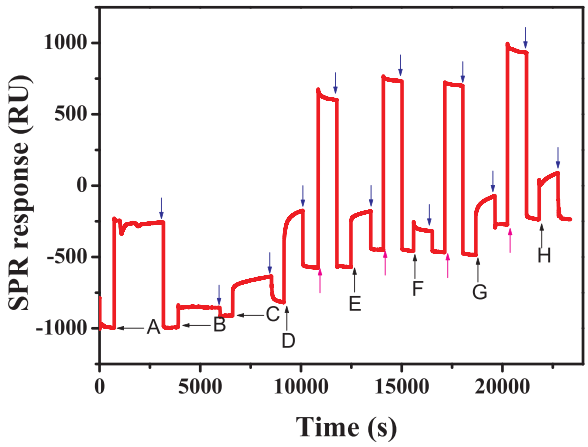

Fig. 5. SPR response for detection DENV. EDC-NHS (point A), antibody (point B), BSA (point C), pool DENV (point D), pool DENV (point E), negative control with zika virus (point F), pool DENV (point G) and negative control with zika virus (point H). All washing steps of experiment were performed using PBS pH 7.4 represented by the blue arrows down (↓) and every step of regenerating the sensor surface was performed using glycine-HCl solution represented by the pink arrows up (↑).

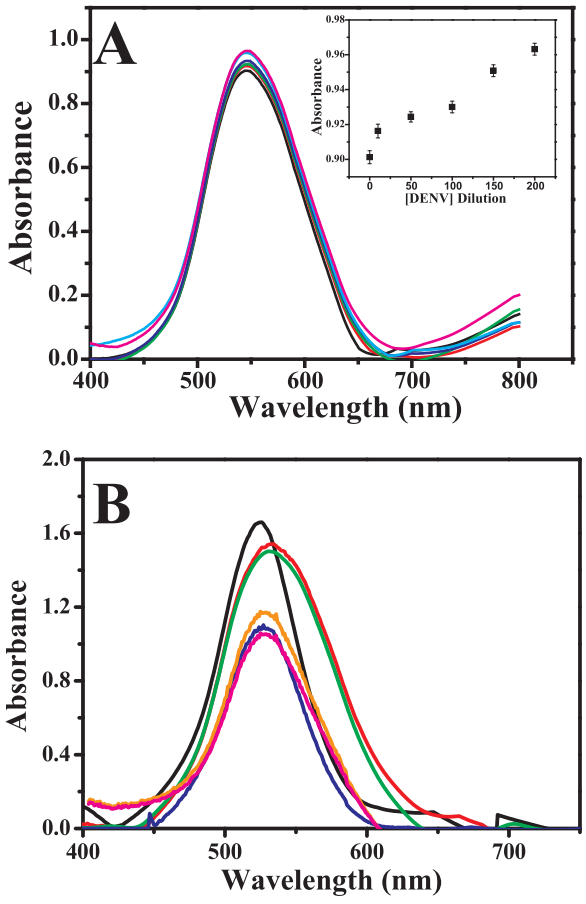

Fig. 6. A) Variations of pool DENV concentrations. A sample pool DENV at titre 10^7 $TCID_{50}$/mL diluted to 0.0 µL PBS (black line), 1/10 µL PBS (red line), 1/50 µL PBS (green line), 1/100 µL PBS (blue line), 1/150 µL PBS (pink line) and 1/200 µL PBS (violet line). Insert in figure calibration curve for pool DENV. B) UV–Vis absorbance spectra of control negative. AuNPs (black line), MUA (red line), EDC-NHS (green line), antibody (blue line), ZIKV (orange line) and YFV (pink line).

that the absorbance spectrum of AuNPs exhibited a decrease in the absorbance at the peak wavelength as a function of the concentration of DENV (Fig. 6A). The inset shows that a linear fit to the plot of the absorbance as a function of refractive index gives a detection limit of $TCID_{50}$ 10^7 with a linear range dilution from 0.0 to 200.0 and linear response $R = 0.993$. The detection limit of $TCID_{50}$ 10^7 is within the clinically relevant range for humans, since according to the literature viraemia is considered as positive for a titre $\geq 10^{1.7}$ $TCID_{50}$ (Murgue et al., 2000). All experiments were made in triplicate. The relative standard deviation (RSD) is 6.0%, showing a good reproducibility of the immunosensor preparation. Stability is a key factor for future application. In order to verify if over time there were changes in the values measurements were performed 15 to 15 days in the course of two month. The answer response decreases slightly in the first few days, and afterward, the response tends to be practically constant and retained 91% of its original response over two months of storage. The slow

decrease in response seemed to be related to the gradual deactivation of the immobilized antibody incorporated in the nanoparticles.

Also, we evaluated the detection of viruses in the presence of potential interferences that may be present in the viral culture process. The ZIKV and Yellow Fever (YFV) virus interference was tested to assess the specificity of our assay in detecting the dengue virus and in ensuring the efficacy of the experiment, because both virus could provide a false positive response and invalidate the herein found results. The LSPR spectrum of ZIKV and YFV is shown in Fig. 6B, wherein the antibody was labeled as AuNP (blue line) after the addition of the interferer ZIKV (orange line) and YFV. It was possible observing displacement in the wavelength and absorbance peak reduction by comparing the results; it showed modifications in the surface at wavelength 527 nm and at absorbance 1.07 until the antibody. When ZIKV or YFV was added to the solution, unlike the dengue virus there was no wavelength displacement at 526 nm, thus there was no virus binding with the AuNPs-antibody complex. We also tested BSA as possible interference. Upon addition of 100 fold excess of BSA, our sensor did not show any kind of absorbance increase. These results proved that the presence of other similar viruses or a generic protein did not affect the selectivity of the methodology in detecting only the dengue virus, and it evidenced the efficiency of the immunosensor.

All dengue serotypes were analyzed through the traditional RT-qPCR and ELISA techniques to validate the results found in the present experiment. It found 99.0% reproducibility in comparison to our results. All analyses in the current study were performed in triplicate. The new methodology simplicity provides distinct advantages over other dengue detection methods. The assay can be packaged as a pre-mixed reaction solution in Eppendorf tubes, and may be performed without any specialized training. Furthermore, this assay is inexpensive, costing about $3 per sample, as compared to serological testing or PCR-based methods which can cost $10 per sample. Assay components are stable at room temperature, and exhibit stability and sensitivity at temperatures greater than 30 °C.

4. Conclusion

The results presented in this work, designed to be active against all forms of dengue virus and is capable of effectively detecting the dengue virus. Coupling antibody with gold nanoparticle aggregation provides an attractive alternative detection approach for DENV detection. This new methodology involves simple operational procedures, significantly reducing its testing duration from around 1–3 days to less than 5 min, making it faster than traditional clinical methods. Detection prior to the onset of symptoms could allow a more effective diagnosis and treatment of infected patients, and a fast recovery from the disease. Full development of this detection assay would greatly enhance virus diagnostics and epidemiology by providing an assay that is more rapid, easier to use, has greater portability than current detection methods.

Acknowledgments

The authors thank FAPESP (2016/159191-8), CAPES and CNPq (304581/2016-0) Brazil, for the grants and the financial support to this work.

Appendix A. Supporting information

Supplementary data associated with this article can be found in the online version at http://dx.doi.org/10.1016/j.virol.2017.10.001.

References

Basso, C.R., Tozato, C.C., Araujo Junior, J.P., Pedrosa, V.A., 2015. Anal. Methods 7, 2267.
Cao, X.D., Ye, Y.K., Liu, S.Q., 2011. Anal. Biochem. 417, 16.
Cordeiro, M., Carlos, F.F., Pedrosa, P., Lopez, A., Baptista, P.V., 2016. Diagnostics 6, 20.
De Feijter, J.A., Brenjsamins, J., Veer, F.A., 1978. Biopolymers 17, 1759.
Endo, T., Kerman, K., Nagatani, N., Takamura, Y., Tamiya, E., 2005. Anal. Chem. 77, 6984.
Frens, G., 1973. Nat. Phys. Sci. 241, 20.
Gromowski, G.D., Roehrig, J.T., Diamond, M.S., Lee, J.C., Pitcher, T.J., Barrett, A.D., 2010. Virology 407, 246.
Guzman, M.G., Kouri, G., 2004. Int. J. Infect. Dis. 8, 80.
Haes, J., Chang, L., Klein, W.L., Duyne, R.P.V., 2005. J. Am. Chem. Soc. 127, 2271.
Jahanshahi, P., Zalnezhad, E., Sekaran, S.D., Adikan, F.R.M., 2014. Sci. Rep. 4, 7.
Kaur, K., Forrest, J.A., 2012. Lagmuir 28, 2736.
Kumbhat, S., Sharma, K., Gehlot, R., Solanki, A., Joshi, V., 2010. J. Pharm. Biomed. Anal. 52, 259.
Li, Y., Lee, H.J., Corn, R.M., 2007. Anal. Chem. 79, 1088.
Liu, C., Jia, Q., Yang, C., Qiao, R., Jing, L., Wang, L., Xu, C., Gao, M., 2011. Anal. Chem. 83, 6784.
Liu, P., Yang, X., Sun, S., Wang, Q., Wang, K., Huang, J., Liu, J., He, L., 2013. Anal. Chem. 85, 7695.
Ma, Z., Sui, S.F., 2002. Angew. Chem. 41, 2179.
Murgue, B., Roche, C., Chungue, E., Deparis, X., 2000. J. Med. Vir. 60, 438.
Nunes, M.R.T., NunesNeto, J.P., Casseb, S.M.M., Nunes, K.N.B., Martins, L.C., Rodrigues, S.G., Matheus, S., Dussart, P., Casseb, L.M.N., Vasconcelos, P.F.C., 2011. J. Virol. Methods 171, 20.
Pelton, M., Aizpurua, J., Bryant, G., 2008. Laser Photon. Rev. 2, 159.
Ramos-Castañeda, J., Santos, F.B., Martínez-Vega, R., Araujo, J.M.G., Joint, G., Sarti, E., 2017. PLoS Negl. Trop. Dis. 11, 24.
Reed, L.J., Muench, H., 1938. Am. J. Epidemiol. 27, 497.
Rica, R.D.L., Stevens, M.M., 2012. Nat. Nanotechnol. 7, 824.
Saxena, P., Dash, P.K., Santhosh, S.R., Shrivastava, A., Parida, M., Rao, P.L., 2008. Virol. J. 5, 5.
Tang, D.P., Cui, Y.L., Chen, G.A., 2013. Analyst 138, 981.
Urdea, M., Penny, L.A., Olmsted, S.S., Giovanni, M.Y., Kaspar, P., Shepherd, A., Wilson, P., Dahl, C.A., Buchsbaum, S., Moeller, G., Burgess, D.C.H., 2006. Nature 444, 79.
Vaculovicova, M., Michalek, P., Krizkov, S., Macka, M., Adam, V., 2017. Anal. Methods 9, 2391.
Verdoodt, N., Basso, C.R., Rossi, B.F., Pedrosa, V.A., 2017. Food Chem. 221, 1796.
Wang, C., Irudayaraj, J., 2008. Small 4, 2208.
Wang, L., Li, J., Song, S., Li, D., Fan, C., 2009. J. Phys. D Appl. Phys. 42, 11.
Wang, S.M., Sekaran, S.D., 2010. Am. J. Trop. Med. Hyg. 83, 695.
Wiwanitkit, S., Wiwanitkit, V., 2015. Nanomedicine 12, 249.
World Health Organization. ⟨http://www.who.int/mediacentre/factsheets/fs117/en/⟩. Acessed 19 January 2017.
Xianyu, Y., Wang, Z., Jiang, X., 2014. ACS Nano 12, 12747.
Zhang, B., Salieb-Beugelaar, G.B., Mutro, N.M., Weidmann, M., Hunziker, P., 2015. Nanomedicine 11, 1761.
Zhao, H., Brown, P.H., Schuck, P., 2011. Biophys. J. 100, 2309.